

# Effects of Thermo-Mechanical Loads on Aeroelastic Instabilities of Metallic and Composite Panels

*Erasmus Carrera*<sup>1,2</sup>, *Maria Cinefra*<sup>1</sup>, *Enrico Zappino*<sup>1\*</sup>, *Lorenzo Succi*<sup>1</sup>

1. Department of Mechanical and Aerospace Engineering, Politecnico di Torino,  
Corso Duca degli Abruzzi 24, 10129 Torino, Italy;

2. School of Aerospace, Mechanical and Manufacturing Engineering, RMIT University, Melbourne, Australia

(Received 22 October 2013; revised 16 November 2013; accepted 30 November 2013)

**Abstract:** Panel flutter phenomena can be strongly affected by thermal loads, and so a refined aeroelastic model is presented. Higher-order shell theories are used as structural models. The aerodynamic forces are described using the Piston theory. The temperature is considered uniform over the thickness of the panel. The aero-thermo-elastic model is derived in the framework of the Carrera unified formulation (CUF), therefore the matrices are expressed in a compact form using the "fundamental nuclei". Composite and sandwich structures are considered and different boundary conditions are taken into account. The effects of the thermal load on the aeroelastic behavior are investigated.

**Key words:** Carrera unified formulation (CUF); panel flutter; aeroelasticity; aero-thermo-elasticity; shell elements

**CLC number:** O325

**Document code:** A

**Article ID:** 1005-1120(2014)02-0128-05

## 1 Introduction

Panel flutter is an aeroelastic phenomena that can cause failure of panels of wings, fuselages, and missiles. The panel flutter phenomena involves mainly the aeronautic structures but it appears also on space structure during the coasting phase. The new launcher generations try to improve the performance by introducing new panels, and they must protect the cryogenics stage during the coasting phase. These panels, called the versatile thermal insulation (VTI) panels, are bigger than the common aeronautical panels and usually are connected with the main structure by means of pinched points. The dimension, the boundary conditions (BCs) and the weight requirements make the VTI panels very flexible and so they may easily occur in aeroelastic phenomena. The aerodynamic heating on the external surface and the cryogenic fluid on the inner surface, create a high thermal gradient along the thickness of the panel. The stress field due to the differen-

tial thermal loads could strongly affect the dynamic behavior of the panel and can play an important role in the aeroelastic instability, as shown by Dixon et al<sup>[1]</sup>.

The analysis of composite structures subjected to thermal loads is a challenging problem and many works were presented on this topic. A valuable example are the works by Noor and Burton<sup>[2]</sup>, as well as Khdeir<sup>[3]</sup>. Carrera<sup>[4-5]</sup> proposed the use of advanced structural models in the thermo-mechanical analysis of composite panels in order to introduce a more refined solution over the panels thickness. The improvements introduced by the use of refined models allow a non-constant temperature profile to be considered obtaining accurate results, as shown in Ref. [5]. More recent application of higher-order shell models to the thermo-mechanical analysis are those by Wu and Chen<sup>[5]</sup>, as well as Fazzolari and Carrera<sup>[6]</sup>.

In this paper, an aero-thermo-mechanical analysis is performed using a refined shell theory<sup>[7]</sup> for the structural model including the ther-

\* **Corresponding author:** Enrico Zappino, Research student, E-mail: enrico.zappino@polito.it.

mal effects and the Piston theory<sup>[8]</sup>, in its linear form, for the aerodynamic loads. A cylindrical shell finite element derived by means of the Carrera unified formulation (CUF)<sup>[9]</sup> is adopted. The higher-order models derived by means of the CUF approach allow the thermo-mechanical problem to be addressed with very high accuracy. Different material laminations are considered; isotropic, composite, and sandwich material. Only supersonic regimes are investigated. The results show that the thermal loads can afflict the aeroelastic behavior of the panel. The results also show the effect of the use of the refined shell elements respect to the classical one. The advantages of these models are pointed out mainly in the composite and sandwich panels.

## 2 Aeroelastic Model

The aeroelastic model used in the present work can be derived imposing the equilibrium of the work virtual variations. The principle of virtual displacement (PVD) states that

$$\delta L_{\text{int}} + \delta L_{\text{ine}} = \delta L_{\text{aer}} + \delta L_{\text{heat}} \quad (1)$$

where  $L_{\text{int}}$  is the work due to the elastic forces,  $L_{\text{ine}}$  the inertial work,  $L_{\text{aer}}$  the work made by the aerodynamic forces, and  $L_{\text{heat}}$  the thermal work.  $\delta$  denotes the virtual variation. If the solution is supposed to be harmonic and the contributions are expressed in a matrix form, the previous Eq. (1) becomes

$$\left[ -\omega^2 \mathbf{M} + i\omega \mathbf{D}_a + (\mathbf{K} + \mathbf{K}_a + \mathbf{K}_{\text{heat}}) \right] \{\bar{\mathbf{q}}\} e^{i\omega t} = 0 \quad (2)$$

From left to right, it is possible to see the mass matrix of the structure  $\mathbf{M}$ , the aerodynamic dumping matrix  $\mathbf{D}_a$ , the structural stiffness matrix  $\mathbf{K}$ , the aerodynamic stiffness matrix  $\mathbf{K}_a$ , and finally the thermal stress matrix  $\mathbf{K}_{\text{heat}}$ . The matrices are derived in terms of fundamental nuclei, a  $3 \times 3$  matrix that is independent of the used model. The CUF approach is used both for structural and aerodynamic matrices. More details on CUF can be found in Refs. [9-10].

### 2.1 Unified formulation

The generic three-dimensional (3D) displacement model can be written as

$$u(x, y, z) = f(x, y, z; t) \quad (3)$$

The 3D formulation can be reduced to the two-dimensional (2D) formulation by introducing the function  $F_\tau$ . This function introduces an expansion over the thickness of the structure. Therefore the displacement field can be written as

$$u(x, y, z) = u_\tau(x, y; t) F_\tau(z) \quad \tau = 1, 2, \dots, N \quad (4)$$

where  $F_\tau$  is a function expansion used to approximate the displacement over the thickness of the structure. The formulation of the expansion can be assumed by using an equivalent single layer (ESL) approach or in a layer wise (LW) formulation (see Ref. [9]). The former approach uses a global approximation over the thickness, and the latter is able to provide a local description introducing an expansion over each layer. The finite element method (FEM) approach is used to solve the problem over the reference surface. By introducing the shape functions  $N_i$ , the displacements can be written in the following formulation

$$u(x, y, z) = q_{i\tau}(t) N_i(x, y) F_\tau(z) \quad \tau = 1, 2, \dots, K$$

where  $N_i$  are the Lagrange functions and  $K$  is the number of node of the used element.

### 2.2 Elastic work

The elastic work can be derived by the classical formulation of stress and strain

$$\varepsilon = \mathbf{D}u; \quad \sigma = \mathbf{C}\varepsilon$$

The expression of  $\mathbf{D}$  can be found in Ref. [11]. The components of  $\mathbf{C}$  are the material coefficients whose explicit expressions are not reported here for the sake of brevity, they can be found in Ref. [5]. The internal work can be written as

$$\delta L_{\text{int}} = \int_V (\delta \boldsymbol{\varepsilon}^T \boldsymbol{\sigma}) dV = \delta q_{i\tau}^T \left[ \int_V [\mathbf{D}^T (N_i F_\tau I)] \mathbf{C} [(N_i F_\tau I) \mathbf{D}] dV \right] \delta q_{js} = \delta q_{i\tau}^T \mathbf{K}^{ijrs} \delta q_{js} \quad (5)$$

### 2.3 Inertial work

The mass matrix formulation derives from the variation of the work made by the inertial forces

$$\delta L_{\text{ine}} = \int_V (\delta \mathbf{u}^T \rho \ddot{\mathbf{u}}) dV = \delta q_{i\tau}^T \left[ \int_V [(N_i F_\tau I)] \rho [(N_j F_s I) dV] \right] \delta q_{js} =$$

$$\delta q_{ic}^T \mathbf{K}^{ijrs} \delta q_{js} \quad (6)$$

A single dot denotes the derivative with respect to time, therefore, in the case of the displacement vector  $\mathbf{u}$ , double dots denote acceleration.

## 2.4 Thermal work

The strain and the stress fields related to the thermal load is assumed as

$$\boldsymbol{\varepsilon}^h = \alpha_p \Delta \mathbf{T}; \quad \boldsymbol{\sigma}^h = \mathbf{C}_p \alpha_p \Delta \mathbf{T} = \lambda_p \Delta \mathbf{T}$$

where  $\alpha_p$  contains the in-plane thermal expansion coefficients along the  $x$ ,  $y$  and  $xy$  directions,  $\Delta \mathbf{T}$  is a vector ( $3 \times 1$ ) containing the temperature gradient and  $\mathbf{C}_p$  is the in-plane material matrix coefficients. In order to obtain the fundamental nuclei the Von Karman non-linear formulation is used

$$\begin{aligned} \delta L_{\text{heat}} = \int_V (\delta \boldsymbol{\varepsilon}_{xx}^{nlT} \boldsymbol{\sigma}_{xx}^h + \delta \boldsymbol{\varepsilon}_{yy}^{nlT} \boldsymbol{\sigma}_{yy}^h + \delta \boldsymbol{\varepsilon}_{xy}^{nlT} \boldsymbol{\sigma}_{xy}^h) dV = \\ \delta q_{ic}^T \left[ \int_V ((F_\tau N_{i,x} N_{i,x} F_s) \boldsymbol{\sigma}_{xx}^h + \right. \\ \left. (F_\tau N_{i,y} N_{i,y} F_s) \boldsymbol{\sigma}_{yy}^h + (F_\tau N_{i,x} N_{i,x} F_s) \boldsymbol{\sigma}_{xy}^h) dV \right] \delta q_{js} = \\ \delta q_{ic}^T \mathbf{K}_{\text{heat}}^{ijrs} \delta q_{js} \quad (7) \end{aligned}$$

For thin structures, the fundamental nuclei of thermal stress matrix ( $3 \times 3$ ) has only the third diagonal element different from zero, and the other can be assumed negligible. The complete formulation can be found in Ref. [6].

## 2.5 Aerodynamic work

The aerodynamic forces are described using the Piston theory model. Piston theory was introduced for the first time by Ashley and Zartarian<sup>[8]</sup>. It provides an easy formulation of the aerodynamic forces, but it is valid only starting from  $Ma=1.7$  and predicts only coupled mode flutter. Piston theory assumes the pressure distribution as

$$\begin{aligned} \Delta p(y, t) = \frac{2q}{\sqrt{Ma^2 - 1}} \left( \frac{\partial u_z}{\partial y} + \frac{Ma^2 - 2}{Ma^2 - 1} \frac{1}{V} \frac{\partial u_z}{\partial t} \right) = \\ A \frac{\partial u_z}{\partial y} + B \frac{\partial u_z}{\partial t} \quad (8) \end{aligned}$$

The differential pressure is a function of two contributions. The first is caused by the vertical velocity  $\frac{\partial u_z}{\partial t}$ , while the second originates from the slope of the structure in the flow direction  $\frac{\partial u_z}{\partial y}$ . The work due to the aerodynamic forces can be written as

$$\delta L_a = \int_A \delta \mathbf{u} \Delta p d\Lambda = \delta q_{ic}^T \mathbf{K}_{\text{aer}}^{ijrs} \delta q_{js} + \delta q_{ic}^T \mathbf{D}_{\text{aer}}^{ijrs} \delta q_{js} \quad (9)$$

where  $\Lambda$  is the surface exposed at the air flow. The complete formulation has not been reported for sake of brevity.

## 3 Results

In this section are presented the results obtained by using the model introduced in the previous section. The complete aero-thermo-mechanical model is introduced step by step. The first analysis is devoted to the assessment of the mechanical model. Therefore the thermo-mechanical model is introduced. The last example is devoted to the aero-thermo-mechanical analysis of a VTI panel.

### 3.1 Mechanical buckling of a composite panel

A four-layer square panel is considered. The panel has a lateral dimension of 0.1 m and a thickness of 0.002 m. The panel is considered simply supported and the stacking sequence of the lamination is  $[0/90/90/0]$ . The mechanical properties are:  $E_1 = 127.6 \times 10^9$  Pa,  $E_2 = E_3 = 11.3 \times 10^9$  Pa,  $G_{12} = G_{13} = 6.0 \times 10^9$  Pa,  $G_{23} = 1.8 \times 10^9$  Pa,  $\nu_{12} = \nu_{13} = 0.3$ ,  $\nu_{23} = 0.36$ . A second-order layer wise model is used in the analyses. The critical stress  $\sigma_{xx}$  is investigated imposing a constant value of  $\sigma_{yy}$ .

Fig. 1 shows the evolution of the critical load  $\sigma_{xx-cr}$ , at different preload  $\sigma_{yy}$ . The results show that by increasing the preload, the critical load decreases as expected. The numerical results are reported in Table 2, where the reference value presented in Ref. [6] are also reported.

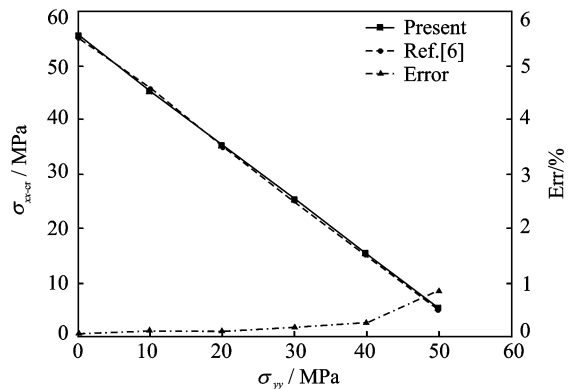


Fig. 1 Evolution of the critical value  $\sigma_{xx}$  at different  $\sigma_{yy}$  preloads

**Table 1** Critical stress load  $\sigma_{xx-cr}$  at different  $\sigma_{yy}$  preloads

$\sigma_{yy}$	$\sigma_{xx-cr}$	$\sigma_{xx}$ [6]
0	55.42	55
10	45.43	46
20	35.43	35
30	25.42	25
40	15.42	15

### 3.2 Thermal buckling of a composite panel

In order to validate the thermo-mechanical solver, a five-layer composite panel with stacking sequence  $[\theta/-\theta/\theta/-\theta/\theta]$  is considered. The reference test case presented in Ref. [6] uses a Ritz/Galerkin approach for evaluating the thermal buckling load and varying the fibers orientation. The panel has the following characteristics; length  $l=1$  m, width  $w=1$  m,  $h=0.01$  m,  $e_1=40 \times 10+9$  Pa,  $e_2=e_3=1 \times 10+9$  Pa,  $G_{12}=G_{13}=0.6 \times 10+9$  Pa,  $G_{23}=0.5 \times 10+9$  Pa,  $\nu_{12}=\nu_{13}=\nu_{23}=0.25$ ,  $\alpha_1=2 \times 10^{-8}$  K $^{-1}$ ,  $\alpha_2=2.25 \times 10^{-5}$  K $^{-1}$ . A second-order LW model is used in the analyses.

As expected, in correspondence of  $\theta$  equal to 0 or 90°, both results obtained using Galerkin and FEM approach, are in good agreement. Varying the fiber orientation, FEM formulation provides more conservative results. It is known that Ritz/Galerkin-based solvers, are less capable of correctly implementing the BCs for angle-ply thin structures. Fig. 2 shows critical temperature trends with both the approaches.

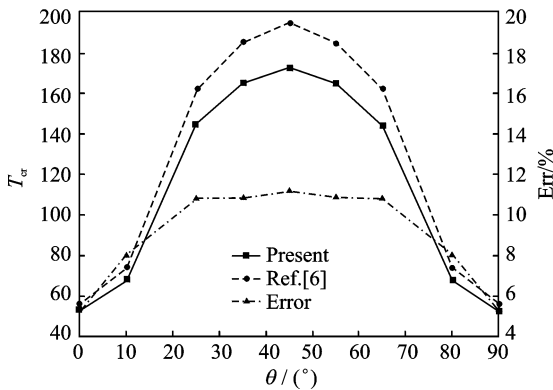


Fig. 2 Critical temperatures vs lamination angles

### 3.3 Aero-thermo-mechanical analysis of VTI panel

Let us consider 1/3 of cylinder arc length VTI sandwich panel. Characteristics of this con-

figuration are;  $a=1.5$  m,  $b=3.12$  m,  $h_{tot}=0.012$  m,  $h_{1-skin}=0.0005$  m,  $h_{core}=0.01$  m,  $R=1.49$  m. Core  $-E=5.4 \times 10^{+7}$  Pa,  $G=2.3 \times 10^{+7}$  Pa,  $\nu=0.1739$ ,  $\rho=80$  kg/m $^3$ ,  $\alpha=10^{-6}$  K $^{-1}$ . Skins  $-E_{11}=85.0 \times 10^{+9}$  Pa,  $E_{22}=E_{33}=1.5 \times 10^{+9}$  Pa,  $G_{12}=G_{13}=1.6 \times 10^{+9}$  Pa,  $G_{23}=1.8 \times 10^{+9}$  Pa,  $\nu_{12}=\nu_{13}=0.3$ ,  $\nu_{23}=0.45$ ,  $\alpha_1=0.9 \times 10^{-6}$  K $^{-1}$ ,  $\alpha_2=27.0 \times 10^{-6}$  K $^{-1}$ .

Since this analysis is used an LW theory of the second-order, it corresponds to 2754 degrees of freedom (Dofs). The panel is simply supported along the sides in the span-wise direction. The combined effects of curvature, thickness, and sandwich configuration provides an elevated momentum of inertia of the panel. So, this involves a very high critical temperature, for thermal buckling. The obtained results indicate that  $T_{cr}=17080$  K, which is obviously unrealistic for any current application. Hence, the lower temperature is chosen.

Table 2 shows the critical Mach numbers at different temperatures for a reference density of  $\rho=0.8$  kg/m $^3$ . The temperatures do not have significant effects on the aeroelastic behavior in terms of stability boundary. Applying higher thermal stress, expressed as a fraction of the critical temperature, results notify a relevant reduction of the stability margin, as shown in Table 3.

Fig. 3 shows the modal damping variation for different temperatures.

**Table 2** Critical Mach number at different temperature  $\Delta T$ 

$\Delta T$ /K	0.0	300	400	500
$M_{cr}$	7.55	7.54	7.54	7.54
$F_{cr}$ /Hz	121.15	120.89	120.71	120.63
$\Delta M_{cr}/\%$	—	0.13	0.13	0.13

**Table 3** Critical Mach numbers at different temperatures  $\Delta T/\Delta T_{cr}$ 

$\Delta T/\Delta T_{cr}$	0.0	0.3	0.4	0.5
$M_{cr}$	7.55	4.76	4.15	3.69
$F_{cr}$ /Hz	121.15	96.40	94.05	91.25
$\Delta M_{cr}/\%$	—	36.95	45.03	51.12

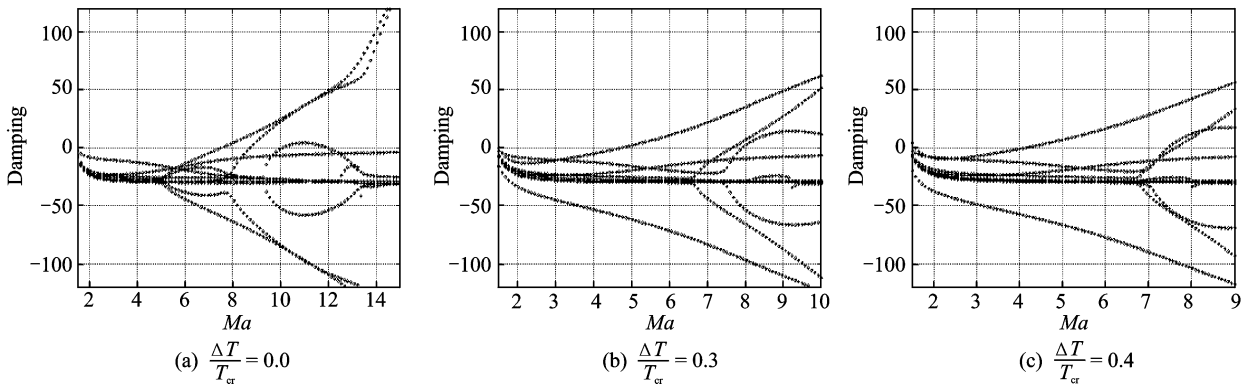


Fig. 3 Modal damping evolution at different temperatures  $\Delta T / \Delta T_{cr}$

## 4 Conclusions

In this paper, an advanced 2D model, derived using the CUF is used to perform the aero-thermo-mechanical analysis of composite panels. The present aeroelastic model shows good agreement with the reference results. The higher-order formulation allows sandwich and composite materials to be investigated. The tests carried out for the VTI panel, shown the influence of the thermal loads on the flutter boundary. Typical operative conditions, with temperature in the operational range of the materials, entail a minimal reduction of the critical Mach, expressed in percentage, compared to the un-stressed condition. Future developments should be devoted to implement a thermal theory, which could represent thermal gradients along the thickness and correctly predict the in-plane stress related to pinched point constraints.

### References:

[1] Dixon S C, Shideler J L, Shore C P. Flutter at Mach 3 of thermally stressed panels and comparison with theory for panel with edge rotational restraint[R]. NASA-TN-D-D3498, 1966.

[2] Noor A K, Burton W S. Computational models for high-temperature multilayered composite plates and shells[J]. Applied Mechanics Reviews, 1992, 45 (10): 419-446.

[3] Khdeir A A. Thermoelastic analysis of cross-ply laminated circular cylindrical shells International Jou-

rnal of Solids and Structures, 1996, 33 (27):4007-4017.

- [4] Carrera E. An assessment of mixed and classical theories for the thermal stress analysis of orthotropic multilayered plates [J]. Journal Thermal Stress, 2000, 23 (9):797-831.
- [5] Carrera E. Temperature profile influence on layered plates response considering classical and advanced theories[J]. AIAA J, 2002, 40 (9):1885-1896.
- [5] Wu Z, Chen W. A global-local higher order theory for multilayered shells and the analysis of laminated cylindrical shell panels [J]. Composite Structures, 2008, 84 (4), pp. 350-361.
- [6] Fazzolari F A, Carrera E. Thermo-mechanical buckling analysis of anisotropic multilayered composite and sandwich plates by using refined variable-kinematics theories [J]. Journal of Thermal Stresses, 2013, 36 (4):321-350.
- [7] Cinfra M, Chinosi C, Della Croce L. MITC9 shell elements based on refined theories for the analysis of isotropic cylindrical structures [J]. Mechanics of Advanced Materials and Structures, 2011.
- [8] Ashley H, Zartarian G. Piston theory—A new aerodynamic tool for the aeroelastician [J]. Composites Structures, 1956:1109-1118.
- [9] Carrera E, Brischetto S, Nali P. Plates and shells for smart structures: classical and advanced theories for modeling and analysis[M]. [S. l.]: John Wiley & Sons, 2011.
- [10] Carrera E, Cinefra M, Petrolo M, et al. Finite element analysis of structures through unified formulation[M]. [S. l.]: John Wiley & Sons, 2014.
- [11] Reddy J N. Mechanics of laminated composite plates and shells. Theory and Analysis[M]. 2nd Ed. [S. l.]: CRC Press, 2004.

